Investigation of solar thermal tides using model data

Didenko, K., Pogoreltsev, A., Koval, A., Ermakova, T.

K. A. Didenko, A. I. Pogoreltsev, A. V. Koval, T. S. Ermakova, "Investigation of solar thermal tides using model data," Proc. SPIE 11916, 27th International Symposium on Atmospheric and Ocean Optics, Atmospheric Physics, 1191687 (15 December 2021); doi: 10.1117/12.2603432

SPIE.

Event: 27th International Symposium on Atmospheric and Ocean Optics, Atmospheric Physics, 2021, Moscow, Russian Federation

Investigation of solar thermal tides using model data

Didenko K.A.[1,2], Pogoreltsev A.I. [1,2], Koval A.V. [1,2], Ermakova T.S. [1,2]

[1]St. Petersburg State University, Saint Petersburg, Russia
[2]Russian State Hydrometeorological University, Saint Petersburg, Russia

ABSTRACT

The study of wave motions in the atmosphere, in particular, atmospheric solar tides is considered in this research. Using the middle and upper atmosphere model (MUAM) data, the latitudinal-high cross-sections of the amplitude and phase of individual tidal components, as well as their temporal variability, were shown. The most suitable periods for the complex Morlet wavelet transform of data were specified for the further use. The results obtained were used to study nonlinear interactions both between atmospheric tides and the mean flow and with each other.
Keywords: planetary waves, atmospheric tides, wavelet transform, nonlinear interaction, potential enstrophy

1 INTRODUCTION

The study of planetary waves propagation into the stratosphere is one of the most important tasks of atmospheric dynamics. This is due to the fact that these waves can influence the general circulation, thermal conditions, as well as the ozone and other chemical distributions. In addition, an amplitude increase of a planetary wave is often observed in the stratosphere during winter, which leads to strong nonlinear phenomena. One of these phenomena is the generation of secondary waves caused by nonlinear wave-wave interaction [1]. Such effects are most clearly manifested during sudden stratospheric warmings (SSWs), which are a strong thermodynamic phenomenon in the winter polar region, affecting the middle atmosphere, causing also significant changes in the mesosphere – the lower thermosphere. Understanding and successfully modeling sudden stratospheric warmings is essential for studying the Earth's climate and improvement long-term forecasts.

This study was based on the idea that in the stratosphere, there is a relationship between changes in the amplitudes of stationary planetary waves (SPWs) with zonal wave numbers m_p=1 and 2 (SPW1 and SPW2). This correlation is mainly due to the nonlinear wave-wave interactions within the stratosphere [2]. Moreover, SPW1 and SPW2 interact with diurnal or semidiurnal migrating tides with zonal wave numbers m_t = 1 and 2. As a result, diurnal and semidiurnal non-migrating tides occur with $m = m_t \pm m_p$ [3]. Furthermore, it is necessary to consider the interaction of tidal components between themselves. The study of forcing reasons and variability of different tidal components in the middle atmosphere is very important for understanding the upper atmosphere dynamics. Specifically, the generation of non-migrating atmospheric tides leads to longitudinal differences in diurnal variation of the vertical wind and affects the hydroxyl emission intensity and the atomic oxygen concentration [4-6].

2 METHODS AND DATA

The method to analyze nonlinear interactions of planetary waves, including solar tides is based on the investigation of conservation of the perturbed potential enstrophy. In this case the terms responsible for nonlinear interactions in the balance equation of the potential enstrophy (Ertel's potential vorticity squared) are calculated. To obtain the balance equation of perturbed potential enstrophy, the conservation equations of Ertel's potential vorticity (EPV) is used and multiplied by perturbed EPV. The general form of the eddy enstrophy balance in log-pressure coordinate system:

$$\frac{\partial}{\partial t}\left(\overline{P'^2}/2\right) = -\overline{P'\left(\overline{V'}\cdot\vec{\nabla}P'\right)} - \overline{P'\left(\overline{V'}\cdot\vec{\nabla}\bar{P}\right)} - \overline{P'\left(\bar{\vec{V}}\cdot\vec{\nabla}P'\right)} + \overline{P'Q'}, \quad (1)$$

where P' and $\bar{P}$ are the perturbed and zonally averaged components of the Ertel's potential vorticity; $\overline{V'}$ and $\bar{\vec{V}}$ are the perturbed and zonally averaged components of wind vector; Q' represents the perturbation of diabatic sources and sinks

27th International Symposium on Atmospheric and Ocean Optics, Atmospheric Physics,
edited by Gennadii G. Matvienko, Oleg A. Romanovskii, Proc. of SPIE Vol. 11916,
1191687 · © 2021 SPIE · 0277-786X · doi: 10.1117/12.2603432

and terms describing the subscale contributions to the momentum equation. The term on the left side of the equation denotes the wave transience and can be defined as a measure of wave activity variability [7]. The first and second terms on the right side describe the wave-wave and wave-mean flow interactions, respectively. The next one term is responsible for the advective transport of potential enstrophy. The last term describes the changes in perturbed enstrophy due to the diabatic heating. This term involves subscale contributions to the momentum equation including momentum deposition by gravity and inertial-gravity waves.

To make the investigation of nonlinear interactions between tidal components possible, it is necessary to obtain the amplitudes and phases of individual tidal components. Time series of amplitudes and phases of standing and eastward/westward propagating planetary waves, including atmospheric tides, were obtained using the complex Morlet wavelet transform.

2.1 Wavelet transform

The model data contain fields of hydrodynamic quantities in the following form: U (x, y, z, t) – zonal wind, V (x, y, z, t) – meridional wind, T (x, y, z, t) – temperature. Time series of amplitudes and phases of individual zonal harmonics for all hydrodynamic quantities are obtained using the Fourier expansion of initial hydrodynamic fields in longitude. Next, the complex Morlet wavelet transform is used, provide time series of amplitudes and phases of standing and eastward/westward propagating planetary waves.

Since the wavelet transform is a bandpass filter with a known response function (the wavelet function), it is possible to reconstruct the original time series using either deconvolution or the inverse filter. In this case, the reconstructed time series is just the sum of the real part of the wavelet transform over all selected scales (periods):

$$x_n(t) = \frac{\delta j \delta t^{1/2}}{C_\delta \psi_0(0)} \sum_{j=0}^{J} \frac{Re\{W_n(s_j)\}}{s_j^{1/2}}, \tag{2}$$

where J is largest scale, δt and δj are the time step and scale step respectively, $Re\{W_n(s_j)\}$ is the real part of the continuous wavelet power spectrum of the time series, s_j – is the corresponding period. The empirical coefficients $C_\delta = 0.776$, $\delta j_0 = 0.6$, $\psi_0(0) = \pi^{-1/4}$ convert the power spectrum to the amplitude spectrum, taking into account the energy scaling [8].

2.2 Tides nonlinear interaction

The received by the method specified in subsection 2.1 amplitudes and phases can be used to analyze nonlinear interactions between migrating atmospheric tides and mean flow as well as between themselves. To obtain the eddy enstrophy balance equation similar to Equation 1 for tides with different zonal wave numbers, it is necessary to take into account the method of secondary planetary waves generation.

In case the signal consisting of two cosine waves with zonal wavenumbers and frequencies (m1, ω1) and (m2, ω2) passes through some quadratic system, the output from this system will contain the secondary waves (2m1, 2ω1), (2m2, 2ω2), (m1–m2, ω1– ω2) and (m1+m2, ω1+ ω2) [9]. Thus, diurnal tide with m_t=1 (DT) is generated as a result of nonlinear interactions of semidiurnal tide (SDT, m_t=2) – DT and eight-hour tide (8hT, m_t=3) with SDT; semidiurnal tide is generated as a result of DT self-interaction and 8hT – DT interaction. As a result, the balance equation for the eddy enstrophy balance of the diurnal and semi-diurnal migrating tides, where the subscripts denote the zonal wave number:

$$\frac{1}{2}\frac{\partial \overline{P_1'}^2}{\partial t} = -\overline{P_1'\left(\overrightarrow{V_1'}\cdot\vec{\nabla}P_2'\right)} - \overline{P_1'\left(\overrightarrow{V_2'}\cdot\vec{\nabla}P_1'\right)} - \overline{P_1'\left(\overrightarrow{V_2'}\cdot\vec{\nabla}P_3'\right)} - \overline{P_1'\left(\overrightarrow{V_3'}\cdot\vec{\nabla}P_2'\right)} - \overline{P_1'\left(\overrightarrow{V_1'}\cdot\vec{\nabla}\bar{P}\right)} - \overline{P_1'\left(\bar{\vec{V}}\cdot\vec{\nabla}P_1'\right)} + \overline{P_1'R_1'}, \tag{3}$$

$$\frac{1}{2}\frac{\partial \overline{P_2'}^2}{\partial t} = -\overline{P_2'\left(\overrightarrow{V_1'}\cdot\vec{\nabla}P_1'\right)} - \overline{P_2'\left(\overrightarrow{V_1'}\cdot\vec{\nabla}P_3'\right)} - \overline{P_2'\left(\overrightarrow{V_3'}\cdot\vec{\nabla}P_1'\right)} - \overline{P_2'\left(\overrightarrow{V_2'}\cdot\vec{\nabla}\bar{P}\right)} - \overline{P_2'\left(\bar{\vec{V}}\cdot\vec{\nabla}P_2'\right)} + \overline{P_2'R_2'}. \tag{4}$$

2.3 MUAM model data

The middle and upper atmosphere model data, available up to 100 km was used for calculations and analysis. An ensemble of solutions was chosen for the neutral El Niño phase conditions and the western phase of the quasi-biennial oscillation, when a strong sudden stratospheric warming (SSW) was observed (simulated). Wave activity and wave interactions usually intensify during this phenomenon. For example, Figures 1 and 2 show the results for January – February. A strong increase in the SPW1 amplitudes occurs at the beginning of January, which is accompanied by a reversal of the zonal mean flow in the stratosphere – Figure 1 upper and middle panels. As a consequence, the sudden stratospheric warming was observed several days later – Figure 1 lower panel. Figure 2 shows the distribution of the amplitudes of SPW2 and SPW3 for the same month. The onset of SSW is preceded by an increase in the amplitudes of SPW2 and 3, as significant as SPW1.

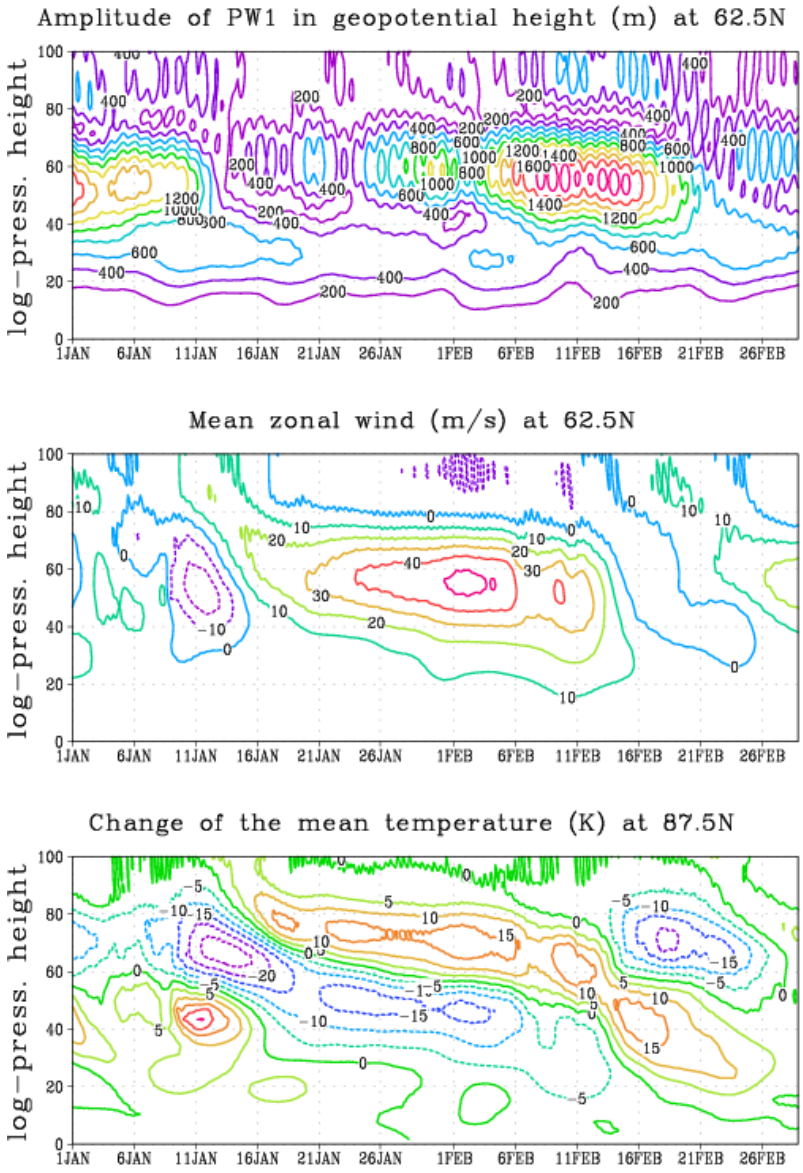

Figure 1. The time-altitude cross-sections of the amplitude of zonal harmonic with $m_p = 1$ in the geopotential height and the mean zonal wind at latitude 62.5°N (upper and middle panels); the change of the zonal mean temperature at 87.5°N (lower panel) for January and February.

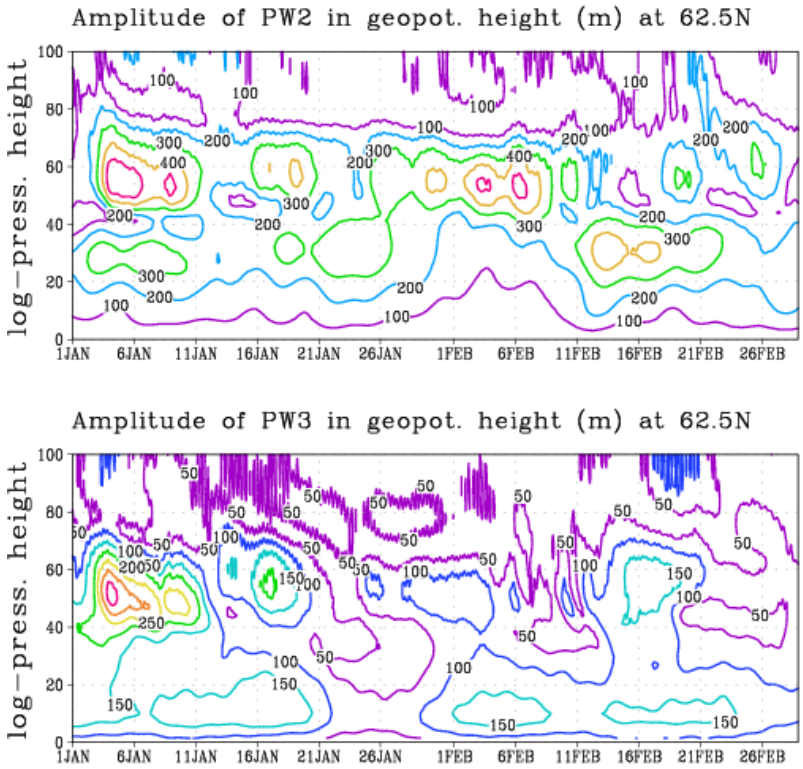

Figure 2. The time-altitude cross-sections of the amplitude of zonal harmonics with $m_p = 2$ (upper panel) and $m_p = 3$ (lower panel) in the geopotential height at latitude 62.5°N for January and February.

3 RESULTS AND DISCUSSION

Time series of amplitudes and phases of temperature, wind components and perturbed component of the Ertel's potential vorticity fields were restored using semiempirical formula (2). Moreover, using the initial and reconstructed fields, latitudinal-high cross-sections of the amplitude and phase of migrating and non-migrating tides were constructed. The data obtained were used to calculate the terms in the Equations 3 and 4.

3.1 Tides intraseasonal variability

The results of temporal variability of the amplitude spectra for temperature are presented in Figures 3-5, MUAM data. A non-migrating tides with m = 1 and 12 hours period, m = 2 and 24 hours period, m = 3 and 12 hours period are also observed in Figures 3-5 (upper panels) respectively. To study the nonlinear interactions between migrating tides, such tides should be filtered (as shown in the lower panels of Figures 3-5). The non-migrating tides generation can be examined separately using filtered amplitudes and phases. Therefore, to restore amplitude and phase of non-migrating tide with m = 1 and 12 hours period 0.3-0.7 period should be specified, for non-migrating tide with m = 2 and 24 hours period – 0.7-1.2 and for m = 3 and 12 hours period – 0.35-0.7.

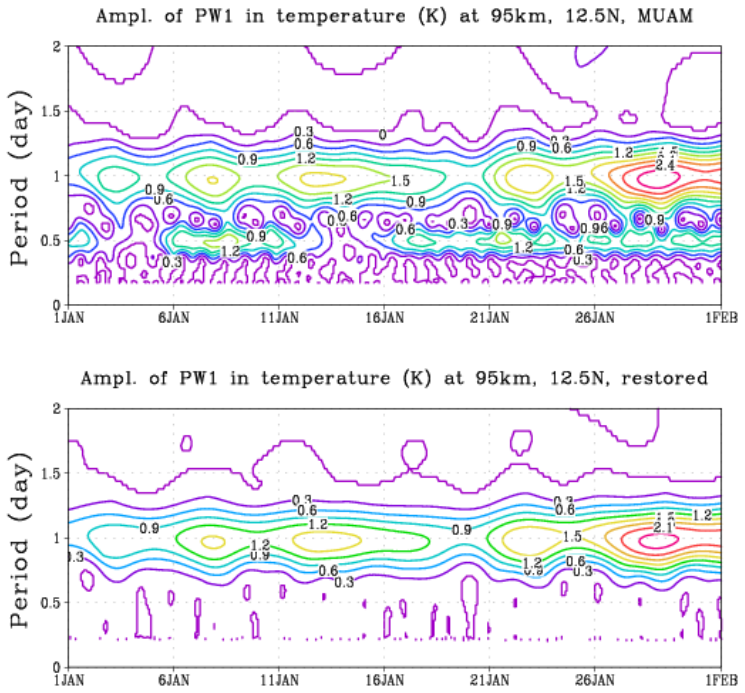

Figure 3. Temporal variability of the diurnal migrating tide at 95 km, 12.5 N, January (upper panel - initial data, lower panel - restored one after wavelet transformation for the interval of 0.7-1.25 periods).

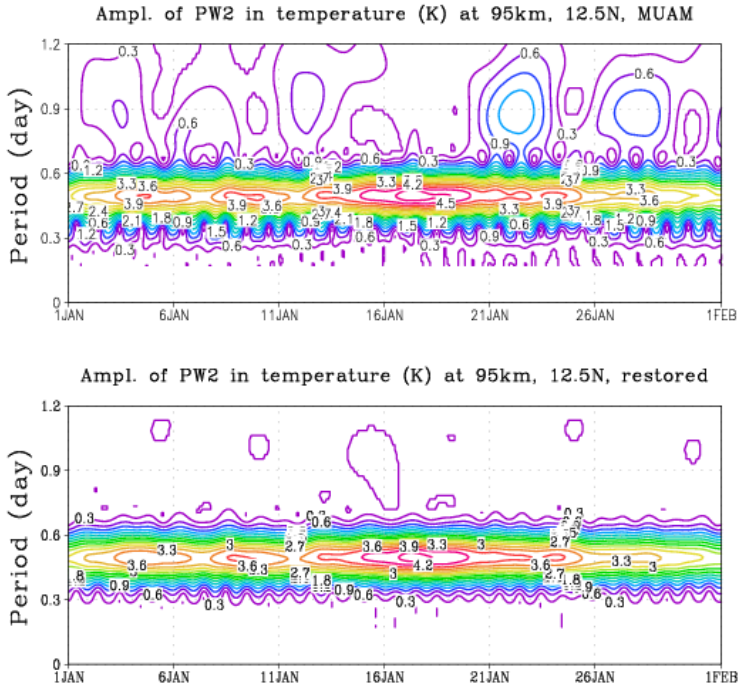

Figure 4. Temporal variability of the semidiurnal migrating tide at 95 km, 12.5 N, January (upper panel - initial data, lower panel - restored one after wavelet transformation for the interval of 0.35-0.7 periods).

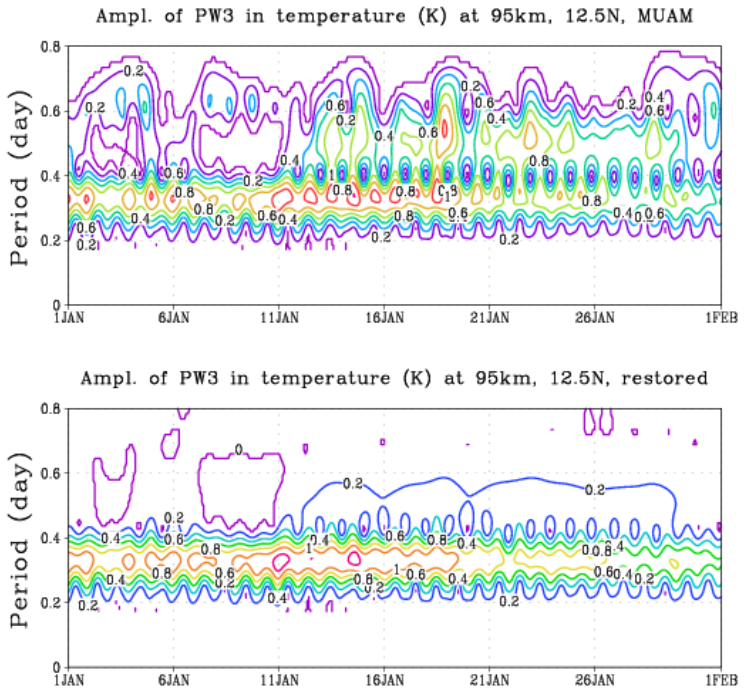

Figure 5. Temporal variability of the 8h migrating tide at 95 km, 12.5 N, January (upper panel - initial data, lower panel - restored one after wavelet transformation for the interval of 0.15-0.45 periods).

The latitudinal-high cross-sections of the amplitude and phase, presented in Figures 6-8, show that the fields of hydrometeorological quantities are perfectly reconstructed using the Morlet wavelet transform with specified intervals. The results provide levels determination, where nonlinear interactions between the tidal components can be analyzed.

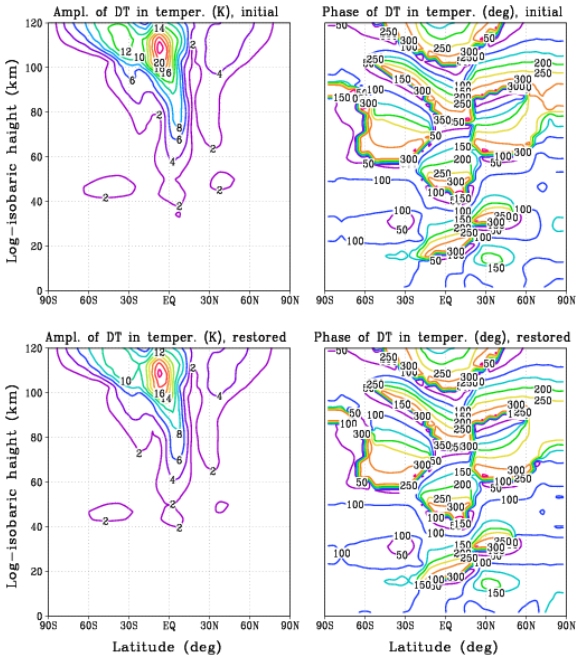

Figure 6. Latitudinal-high cross-sections of the amplitude (left panels) and phase (right panels) for diurnal tide in Kelvin obtained using the initial data (upper panels) and the reconstructed temperature fields (lower panels), January.

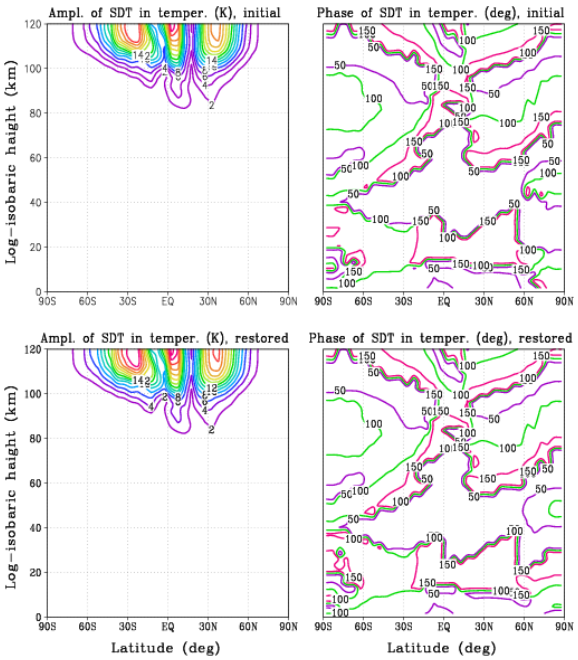

Figure 7. Latitudinal-high cross-sections of the amplitude (left panels) and phase (right panels) for semidiurnal tide in Kelvin obtained using the initial data (upper panels) and the reconstructed temperature fields (lower panels), January.

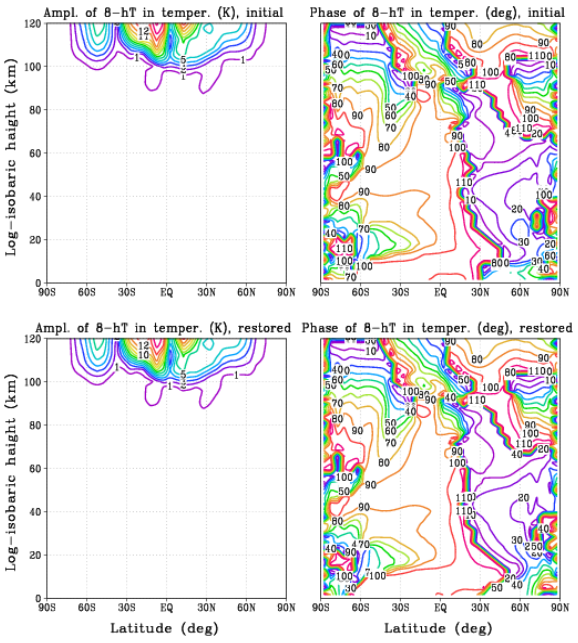

Figure 8. Latitudinal-high cross-sections of the amplitude (left panels) and phase (right panels) for eight-hour tide in Kelvin obtained using the initial data (upper panels) and the reconstructed fields (lower panels), January.

3.2 Terms in eddy enstrophy balance equations

Figures 9-10 show the results of terms calculation in Equations 3 and 4 at 95 km, averaged over the band 52.5-62.5 N using cosine of latitude weighting. Panels (a) show the wave activity variability; (b) and (c) – interaction between migrating tides; (d) – the interaction between the tide and the mean flow. The ordinate values are given in $10^{12}(kg \cdot m^{-3})^2 \cdot PVU^2/day$, where 1PVU (Potential Vorticity Unit) $=10^{-6} \cdot K \cdot m^2 \cdot kg^{-1} \cdot s^{-1}$ units.

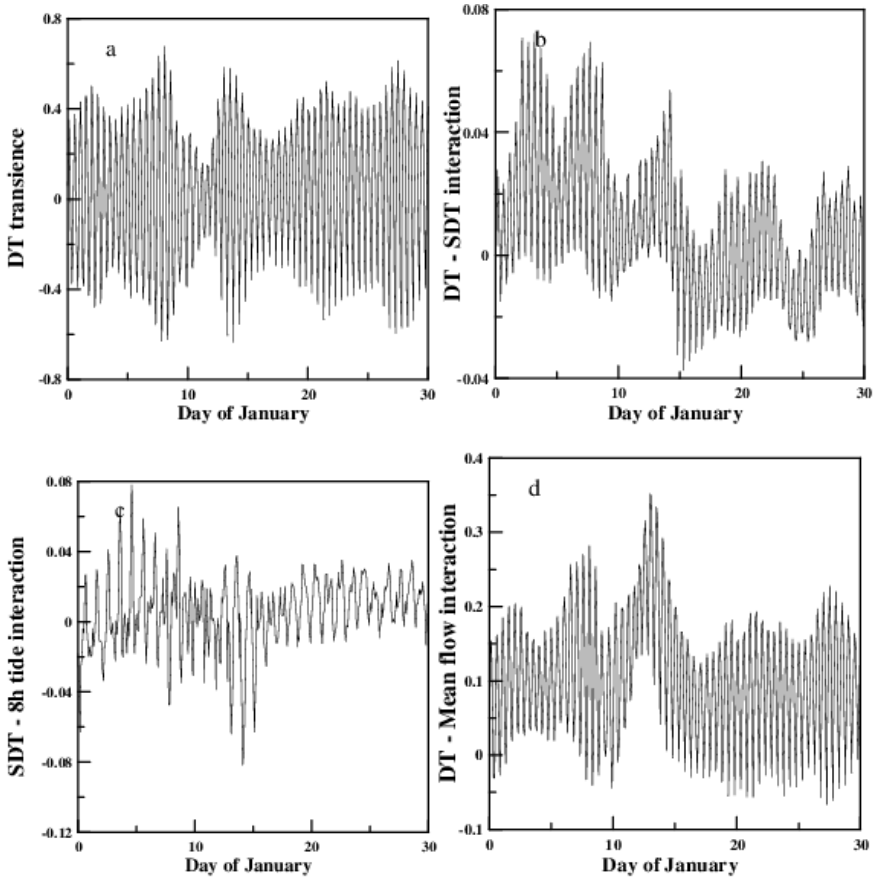

Figure 9. The terms responsible for the contribution to the eddy enstrophy balance (diurnal migrating tide), MUAM data.

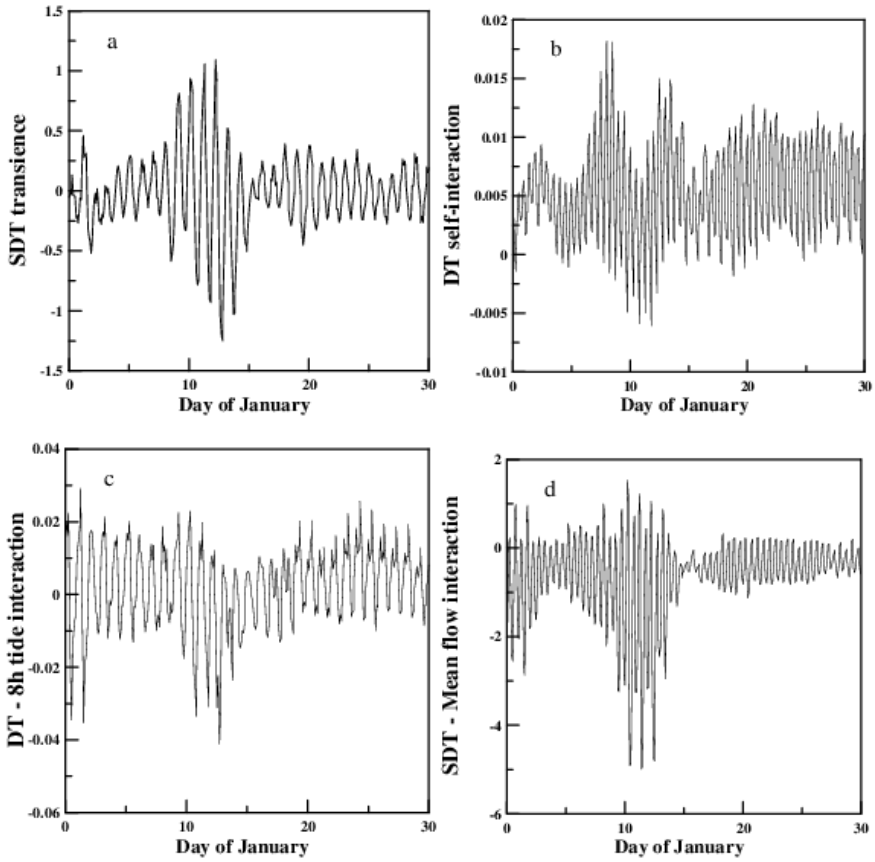

Figure 10. The terms responsible for the contribution to the eddy enstrophy balance (semidiurnal migrating tide), MUAM data.

The results demonstrate that at 95 km altitude the contribution of the terms responsible for the nonlinear interaction between tides is comparable to the contribution of remaining terms. Thus, model data have an advantage over reanalysis data in tidal studies. In addition, the results are influenced by a strong variability of tides, especially diurnal. A decrease in the wave activity of DT is accompanied by an increase of SDT (Figures 9-10, panels (a)) and the changes are observed during the sudden stratospheric warming development. Similar results are obtained when analyzing the wave-mean flow interaction (Figures 9-10, panels (d)). Calculation of wave-wave interactions shows a significant eight-hour tide contribution to the generation of atmospheric tides. It should be noted, that the generation of the diurnal tide is intense before the onset of stratospheric warming, and the semidiurnal one during its development.

4 CONCLUSION

The method to obtain data for calculation nonlinear interactions of atmospheric thermal tides with different zonal wavenumbers and periods is presented in this study. Such an approach is based on the continuous Morlet wavelet transform with specified transform coefficients. The certain intervals of periods for migrating tides as well as non-migrating were determined. The results show that the hydrometeorological quantities fields are perfectly reconstructed using the Morlet wavelet transform with specified intervals of periods (0.7-1.25 for a diurnal tide, 0.25-0.7 for a semidiurnal tide and 0.15-0.45 for an eight-hour tide).

The obtained data were used to analyze nonlinear interactions between migrating atmospheric thermal tides via the eddy enstrophy balance equations. The contribution of the terms responsible for the wave activity variability, the wave-wave interaction and the wave-mean flow interaction was shown. At the mesosphere/lower thermosphere levels, the contribution of different terms to the equation of eddy potential enstrophy is comparable. The contribution of the eight-hour migrating tide to the generation of wave motions is noted. Moreover, strong dynamic phenomena in the stratosphere, such as sudden

warming, are accompanied by a wave activity decrease of the diurnal tide and an increase of semidiurnal one. Such an approach can be applied to non-migrating atmospheric thermal tides studies. This will be the subject of the further research.

Acknowledgments. This research was supported by the Russian Science Foundation under scientific project No. 20-77-10006.

REFERENCES

[1] Didenko, K.A., Pogoreltsev, A.I., Ermakova, T.S. and Shved, G.M. "Nonlinear interactions of stationary planetary waves during February 2016 sudden stratospheric warming", IOP Conf. Ser.: Earth Environ. Sci., 386, 1-7 (2019).
[2] Smith, A.K. "Observation of wave-wave interactions in the stratosphere", J. Atmos. Sci., 40, 2484–2493 (1983).
[3] Pogoreltsev, A.I., Vlasov, A.A., Froehlich, K. and Jacobi, Ch. "Planetary waves in coupling the lower and upper atmosphere", J. Atmos. Solar-Terr. Phys, 69, 2083–2101 (2007).
[4] Medvedeva, I.V., Semenov, A. I., Pogoreltsev, A. I. and Tatarnikov, A.V. "Influence of sudden stratospheric warming on the mesosphere/lower thermosphere from the hydroxyl emission observations and numerical simulations", J. Atmos. Solar-Terr. Phys., 187, 22–32 (2019).
[5] Portnyagin, Y. I., Forbes, J. M., Makarov, N. A., Merzlyakov, E. G. and Palo, S. "The summertime 12-h wind oscillation with zonal wavenumber s = 1 in the lower thermosphere over the South Pole", Ann. Geophysicae, 16, 828 (1998).
[6] Dempsey, S. M., Hindley, N. P., Moffat-Griffin, T., Wright, C. J., Smith, A. K., Du, J. and Mitchell, N. J. "Winds and tides of the Antarctic mesosphere and lower thermosphere: One year of meteor-radar observations over Rothera (68◦S, 68◦W) and comparisons with WACCM and eCMAM", J. Atmos. Solar-Terr. Phys., 212, 1 (2021).
[7] White, I.P., Hua, L., Mitchell, N.J. and Phillips, T. "Dynamical response to the QBO in the Northern winter stratosphere: signatures in wave forcing and eddy fluxes of potential vorticity", J. Atmos. Sci., 72, 4487—4507 (2015).
[8] Torrence, C. and Compo, P.G. "A Practical Guide to Wavelet Analysis", Bulletin of the American Meteorological Society, 79, 65–67 (1998).
[9] Spizzichino, A. "Etude des interactions entre les differentes composantes du vent dans la haute atmosphere", Ann. Geophys., 25(4), 773–783 (1969).